

## Review

## Fourier transform infrared quantification of acid sites in solids: probe molecules in action

Gioele Ancora<sup>1,2,#</sup>, Julio C. Fernandes Pape Brito<sup>1,#</sup>, Ivana Miletto<sup>3</sup>, Leonardo Marchese<sup>2,4</sup>, and Enrica Gianotti<sup>1,\*</sup>

Heterogeneous catalysis plays a crucial role in enabling cleaner and more efficient chemical processes; its performance is largely governed by the nature and strength of active sites. Among these, Brønsted acid sites (BAS) in zeolites are especially important for industrial and emerging sustainable applications. This review discusses recent advances in using Fourier transform infrared spectroscopy with probe molecules to quantitatively assess BAS in zeolites. We highlight a practical and updated workflow emphasizing the determination of reliable molar extinction coefficients for adsorbed probe molecules (carbon monoxide, acetonitrile, ammonia, and pyridine), a key factor often overlooked in acidity measurements. By consolidating methodological developments and best practices, this review provides guidance for improving the accuracy and comparability of acidity quantification in zeolites.

### Through the eyes of infrared spectroscopy: a molecular journey into solid acidity

From industrial transformations to environmental remediation, catalysis shapes our modern world. Among the different types of catalysis, heterogeneous catalysis is central to sustainable chemistry, providing solutions to reduce emissions, valorize waste, and design cleaner processes. At the core of this discipline is the nature and strength of active sites, which govern catalytic activity, selectivity, and efficiency. Accurately quantifying the active sites is essential to understanding how solid catalysts operate and to improving catalyst performance [1–3]. As the world moves toward the 2050 environmental goals, mastering this knowledge is essential for driving innovation in catalysis and advancing the principles of green chemistry [4].

Within the landscape of active sites in heterogeneous catalysts, strong acids, such as Brønsted or Lewis sites, are particularly influential, driving many of the key chemical transformations that underpin modern catalytic processes. Their presence and strength often dictate the reactivity and selectivity of a catalyst, making their identification and quantification central to the rational design of next-generation heterogeneous catalysts [5–8].

Among experimental techniques, **Fourier transform infrared (FTIR) spectroscopy** (see Glossary) is a powerful and versatile method for probing surface acidity in heterogeneous catalysts. Upon adsorption of probe molecules such as carbon monoxide (CO), ammonia (NH<sub>3</sub>), pyridine (C<sub>5</sub>H<sub>5</sub>N), or deuterated acetonitrile (CD<sub>3</sub>CN), characteristic shifts in their vibrational bands provide molecular-level information on the nature, strength, and distribution of Brønsted and Lewis acid sites [9,10]. For instance, the stretching of CO shifts to a higher frequency with respect to the gas phase upon H-bond coordination with **Brønsted acid sites (referred to as BAS, see Glossary)**. Conversely, stronger bases like NH<sub>3</sub> or C<sub>55</sub> are protonated by the BAS, producing IR bands of ammonium or pyridinium species at different wavenumbers from those of the free molecules.

### Highlights

Quantitative Fourier transform infrared assessment of Brønsted acid sites in solids using molecular probes has progressed beyond semiempirical approaches through improved probe selection, spectral analysis, and coupling with quantitative and gravimetric techniques that substantially enhance measurement reliability.

Accurate acidity quantification now relies on the recognition that integrated molar extinction coefficients ( $\epsilon$ ) are probe-, site-, and framework-dependent, overturning the long-held assumption that  $\epsilon$  values are broadly transferable across materials, experimental setups, and analytical protocols.

While recent cross-calibration strategies are enabling more robust and potentially transferable  $\epsilon$  benchmarks, their correct determination and use remain intrinsically

<sup>1</sup>Department for Sustainable Development and Ecological Transition, Università del Piemonte Orientale, Piazza Sant'Eusebio 5, Vercelli 13100, Italy

<sup>2</sup>Department of Science and Technological Innovation, Università del Piemonte Orientale, Viale Teresa Michel 11, Alessandria 15100, Italy

<sup>3</sup>Department of Pharmaceutical Sciences, Università del Piemonte Orientale, Largo Guido Donegani 2, Novara 28100, Italy

<sup>4</sup>Centro di Ricerca e Sviluppo per il Risanamento e la Protezione Ambientale (Centro RisPA), Joint-lab Syensqo/DiSIT, Viale T. Michel 11, Alessandria 15121, Italy

<sup>#</sup>These two authors contributed equally to this manuscript

\*Correspondence: [enrica.gianotti@uniupo.it](mailto:enrica.gianotti@uniupo.it) (E. Gianotti).

Beyond qualitative identification, the semiquantitative or quantitative evaluation of these diagnostic vibrations, achieved through the integration of specific absorption bands, allows one to discriminate between Brønsted and Lewis acid sites, determine their relative populations, and track their evolution under working conditions.

The ability to accurately characterize and quantify acidity is a crucial parameter for elucidating the catalytic properties of solid catalysts. This is particularly relevant for zeolites, heterogeneous catalysts that inherently contain both Brønsted and Lewis acid sites within their inorganic framework. Zeolites are microporous crystalline aluminosilicates with well-defined pore networks. Their  $\text{TO}_4$ -based framework units ( $T = \text{Si}, \text{Al}$ ) create channels and cavities that host catalytically active sites. Owing to the presence of both Brønsted and Lewis acid sites, zeolites display remarkable activity, selectivity, and stability. The synergy between shape selectivity and framework acidity makes zeolites key catalysts in fluid catalytic cracking (FCC) [11], hydrocarbon isomerization, methanol-to-hydrocarbon (MTH) conversion [12], and  $\text{NO}_x$  selective catalytic reduction (SCR) [13]. Their tunable composition, porosity, and acidity also enable sustainable applications, including biomass conversion, fuel cells,  $\text{CO}_2$  capture and conversion, and water treatment, improving energy efficiency and reducing the environmental impact of chemical processes [11,14,15].

The ability to quantify BAS and their acid strength with probe molecules is crucial to understanding zeolites' structure–property relationships and optimizing their catalytic performance.

In this review, we highlight a practical workflow to guide researchers in the quantitative assessment of BAS in zeolites (Figure 1). Particular emphasis is placed on how to determine and apply molar **extinction coefficients** (see Glossary) for different probe molecules, an essential yet often overlooked step that critically affects the reliability of FTIR-derived acidity measurements. By outlining these methodological considerations, we aim to provide a clearer and more consistent framework for quantifying acidity in zeolites and for interpreting structure–property relationships with greater confidence.

### Tools for acid site quantification in solids by probe-molecule adsorption

The BAS quantification in heterogeneous catalysts is a complex procedure, governed by multiple experimental, instrumental, and data-processing variables that determine the accuracy, reliability, and reproducibility of the resulting data.

FTIR quantification of absorbing species in a homogeneous environment is based on the Lambert–Beer law,  $A = \epsilon bC$ , which links absorbance ( $A$ ) to species concentration ( $C$ ,  $\text{mol l}^{-1}$ ) via the molar extinction coefficient ( $\epsilon$ ,  $\text{mol}^{-1} \text{ l cm}^{-2}$  or  $\text{mol}^{-1} \text{ cm}^3$ ) and path length ( $b$ , cm). For solids, however, this relationship must be adapted, since FTIR analysis is typically performed on relatively thick pellets rather than on liquid or gas phases [16]. When probe molecules are adsorbed on the solid surface, the total number of accessible acid sites (BAS or Lewis) can be quantified using a modified Lambert–Beer law, expressed as  $A = \epsilon N \rho$ , where  $A$  is the integrated area ( $\text{cm}^{-1}$ ) of the IR band formed upon probe interaction,  $\epsilon$  is the molar extinction coefficient of the adsorbed species ( $\text{cm } \mu\text{mol}^{-1}$ ),  $N$  is the concentration of the vibrating species ( $\mu\text{mol g}^{-1}$ ), and  $\rho$  is the pellet density (mass/area ratio,  $\text{g cm}^{-2}$ ) [17]. The experimental determination of  $\epsilon$  is reported in Box 1. In addition, sample preparation, applied pressure during pellet formation, particle size, and all parameters affecting the optical path, diffraction, and scattering within the sample (such as specific surface area and particle morphology) affect the  $\epsilon$  values, which can vary significantly among solids [16]. Consequently,  $\epsilon$  must be determined individually for each sample. Serious concerns have also been raised regarding the general applicability of

challenging, requiring careful calibration under well-defined experimental conditions to avoid inconsistencies across the literature.

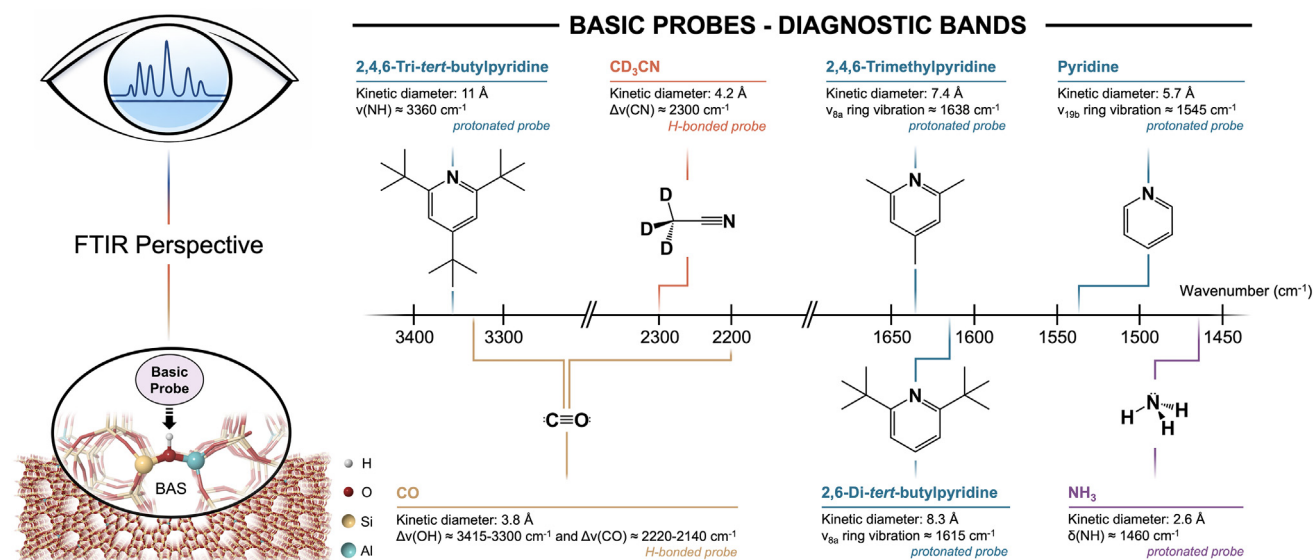
Lambert–Beer-type equations in surface chemistry, as well as the transferability of calculated  $\varepsilon$  between different systems, even when these systems are chemically and/or physically similar [16].

### Probe molecules in action

Suitable **probe molecules** (see Glossary) to monitor surface acidity in zeolites can be identified by evaluating both their proton affinity and their **kinetic diameter** (see Glossary) with respect to the pore aperture of the zeolite framework. For quantitative analysis, where reliable band integration is required, the vibrational modes of probe molecules upon interaction with BAS should not overlap with the intrinsic vibrational features of the zeolite framework and contributions from weak probe–surface interactions. Furthermore, quantitative analysis strongly benefits from the use of FTIR **difference spectra** (see Glossary), obtained by subtracting the spectrum of the sample under vacuum from that recorded after probe adsorption/desorption. This approach yields bands with well-defined baselines, facilitating the subsequent mathematical integration. **Spectral normalization** (see Glossary) is also a crucial step, as it ultimately determines the integrated band areas and the reproducibility and comparability of the resulting data [22]. Finally, depending on the nature of the interaction between the probe molecule and the surface sites, the adsorption can be performed either at room temperature or under variable-temperature conditions. In the following sections, different probe molecules with progressively increasing proton affinity and kinetic diameters will be presented with their typical spectroscopic features.

### Carbon monoxide adsorption

CO, with a proton affinity of  $598 \text{ kJ mol}^{-1}$ , is among the most versatile and sensitive probe molecules to characterize and quantify acid sites in solids by FTIR spectroscopy. Its linear geometry and small kinetic diameter (3.8 Å) enable access to sterically hindered surface regions, making it particularly suitable to monitor both Brønsted and Lewis acid sites [23,24]. Upon adsorption, the  $\text{C} \equiv \text{O}$  stretching vibration becomes highly sensitive to the local electronic



Trends in Chemistry

Figure 1. Overview of the most employed basic probe molecules for FTIR characterization of Brønsted acid sites (BAS) in a zeolite framework. The figure highlights the main quantitative diagnostic IR bands of the selected probes after their interaction with BAS as a function of wavenumber, specifying the interaction mechanism (protonation versus hydrogen bonding), together with molecular structures and kinetic diameters. FTIR: Fourier transform infrared.

### Box 1. Determination of the molar extinction coefficient $\epsilon$

Within the use of basic probe molecules as tools for the semiquantitative analysis of Brønsted acidity in materials of different nature, the molar extinction coefficient  $\epsilon$  plays a pivotal role. An accurate determination of  $\epsilon$  for an appropriate adsorption band of each probe molecule is required, as this value is subsequently introduced into the Lambert–Beer equation adapted for solids. It is therefore necessary to use an IR band that can be employed quantitatively, that is, a band unambiguously associated with the interaction between BAS and the probe molecule (e.g., bands corresponding to the protonated form of the probe, as in the case of  $\text{NH}_3$  or  $\text{C}_5\text{H}_5\text{N}$ ), and located in a spectral region where interfering contributions from other vibrational modes are negligible [16]. Subsequently, a calibration-like relationship must be established by plotting the integrated absorbance of the quantitative band as a function of the probe concentration. The slope of the resulting linear regression is then used as the value of the molar extinction coefficient. In this context, since the early 1990s, the quantitative determination of infrared extinction coefficients has been predominantly based on transmission IR spectroscopy. The seminal work of Emeis introduced the concept of integrated molar extinction coefficient (IMEC) IMECs through  $\text{C}_5\text{H}_5\text{N}$  adsorption, assuming that the IMEC does not depend on the material's nature or the strength of the acid site [9]. Subsequent studies refined this approach while highlighting its limitations: Morterra *et al.* [16], and Jentoft *et al.* [18] demonstrated the system-specific nature of adsorption coefficients, strong dependencies on particle size, morphology, and scattering effects.

More recent studies have explored alternative methodologies for the determination of  $\epsilon$ . Glorius *et al.* proposed an approach based on *in situ* diffuse reflectance infrared Fourier transformed (DRIFT) spectroscopy, yielding extinction coefficients in very good agreement with literature values and providing a valuable starting point for further methodological developments [19]. Other contributions, notably by F. Thibault-Starzyk *et al.* [20,21], significantly improved the accuracy of  $\epsilon$  by employing coupled IR/thermogravimetric setups (AGIR), which enable the simultaneous acquisition of both qualitative and quantitative information through the combined use of thermogravimetric analysis and operando IR spectroscopy, complemented by online mass spectrometry. Regardless of the specific methodology, a common and unavoidable requirement remains the determination of  $\epsilon$  on a material-by-material basis, as the transferability of extinction coefficients is intrinsically limited [16].

environment, resulting in characteristic frequency shifts (typically in the range of  $2140\text{--}2220\text{ cm}^{-1}$ ) that directly reflect the strength and nature of the adsorption site [25]. The adsorbed CO bands are well separated from the gas-phase vibration at  $2143\text{ cm}^{-1}$ , which facilitates unambiguous spectral deconvolution and quantitative analysis. When coordinated to Lewis acid sites, such as exposed metal cations in oxides or zeolites, CO donates electron density from its filled  $5\sigma$  orbital to the empty orbitals of the cation. Simultaneously,  $\pi$ -back donation from metal d orbitals to the CO  $\pi^*$  antibonding orbital weakens the  $\text{C}\equiv\text{O}$  bond, producing a redshift or blueshift depending on the cation's oxidation state and electrophilicity [23]. In oxides containing highly electrophilic centers (e.g.,  $\text{Al}^{3+}$ ,  $\text{Zn}^{2+}$ , and  $\text{Fe}^{3+}$ ), the interaction is dominated by  $\sigma$ -donation and yields blue-shifted bands up to  $2220\text{ cm}^{-1}$ , while transition metals capable of significant back-donation (e.g.,  $\text{Cu}^+$  and  $\text{Ni}^{2+}$ ) cause redshifts below  $2140\text{ cm}^{-1}$  [26]. The magnitude of this shift ( $\Delta v_{(\text{CO})} = v_{\text{ads}} - v_{\text{gas}}$ ) provides a quantitative descriptor of Lewis acidity, correlating with the polarization strength of the metal center. This principle was elegantly demonstrated by Maleki and Pacchioni [27], who showed through density functional theory (DFT) calculations that CO adsorption on undercoordinated  $\text{Zr}^{4+}$  sites on monoclinic and tetragonal  $\text{ZrO}_2$  produces blueshifts between  $+12$  and  $+29\text{ cm}^{-1}$  relative to CO gas phase, consistent with experimental results near  $+31\text{--}51\text{ cm}^{-1}$ . Such correlation validates the direct link between  $\Delta v_{(\text{CO})}$  and the local electron-acceptor ability of surface cations. In mesoporous [Al]-SBA-15, upon CO adsorption at 100 K, multiple bands corresponding to distinct families of Brønsted and Lewis sites are observed [23]. Blue-shifted bands at  $2160\text{--}2175\text{ cm}^{-1}$  were attributed to CO bound to framework  $\text{Al}^{3+}$  centers, while lower-frequency bands reflected interactions with surface hydroxyls.

Although CO interacts preferentially with Lewis acid sites, it can also serve as a sensitive probe for Brønsted acidity at cryogenic temperatures. In the seminal FTIR study by Chakarova and Hadjiivanov [24], adsorption of CO at 100 K on H-ZSM-5 led to the formation of H-bonded CO–BAS complexes, giving rise to two red-shifted O–H stretching components at  $3306$  and  $3415\text{ cm}^{-1}$  with respect to the free BAS at  $3616\text{ cm}^{-1}$ , accompanied by a  $\nu_{(\text{C}\equiv\text{O})}$  band at

### Glossary

**Brønsted acid site (referred as BAS):** framework hydroxyl group (e.g.,  $\text{Si-O(H)-Al}$ ) that acts as a proton donor upon interaction with an adsorbed base. In FTIR spectroscopy, BAS are quantified through characteristic vibrational bands of hydrogen-bonded or protonated probe molecules.

**Difference spectra:** infrared spectra obtained by subtracting the spectrum of the activated material from that recorded after probe adsorption/desorption. This procedure suppresses framework contributions, improves baseline quality, and isolates probe-induced vibrational features.

**Extinction coefficients ( $\epsilon$ ):** integrated molar absorption coefficient correlating the integrated area of a vibrational band to the amount of adsorbed species. In solid-state FTIR,  $\epsilon$  is required for quantitative analysis via the modified Lambert–Beer law and is probe-, site-, and material-dependent.

**Fourier transform infrared (FTIR)**

**spectroscopy:** Fourier transform infrared spectroscopy, a vibrational technique used to identify and quantify surface species through their characteristic absorption bands. In acidity measurements, FTIR monitors interactions between molecular probes and acid sites.

**Kinetic diameter:** effective molecular size governing diffusion through porous materials. In zeolites, the kinetic diameter of a probe determines whether it can access internal cavities or selectively interact with external acid sites.

**Probe molecules:** molecules intentionally adsorbed to investigate surface acidity. Common probes (e.g., CO,  $\text{CD}_3\text{CN}$ ,  $\text{NH}_3$ , and  $\text{C}_5\text{H}_5\text{N}$ ) cover a broad range of basicity and molecular size, enabling selective interaction with different types of acid sites.

**Spectral normalization:** data-processing step in which spectra are scaled to a reference signal, such as pellet thickness or a framework vibration. Normalization affects integrated band areas and must be explicitly reported in quantitative analyses.

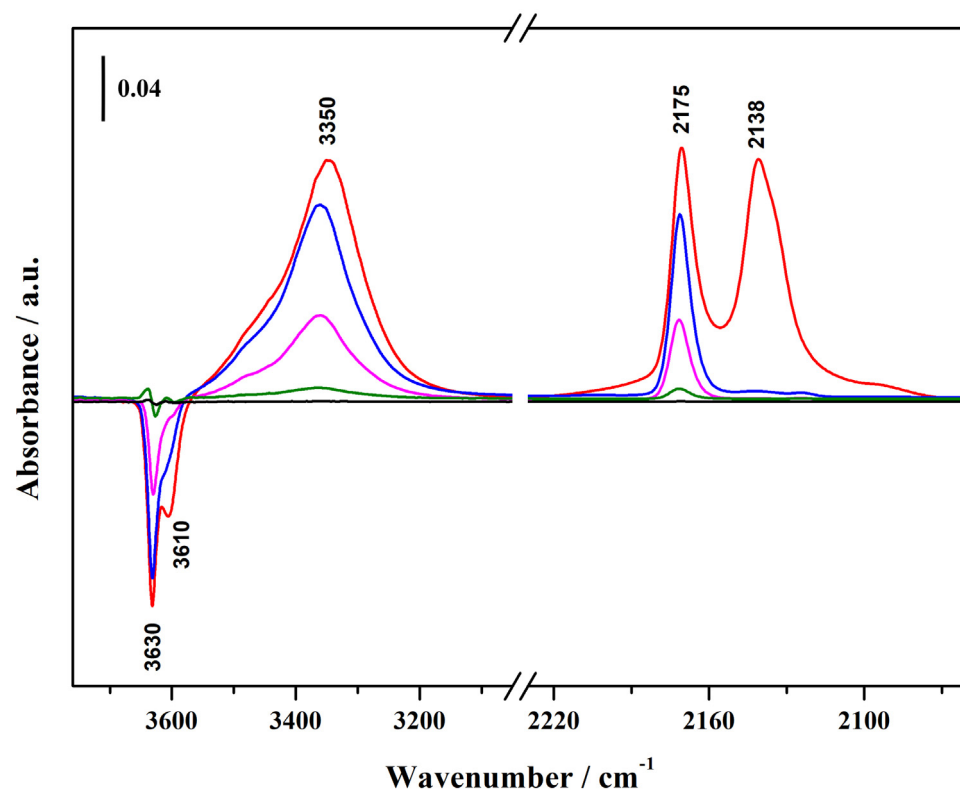
**Zeolite framework codes:** three-letter code (e.g., MFI, FAU, MOR, BEA, and CHA) assigned by the International Zeolite Association to describe framework topology and pore architecture, which strongly influence

2175  $\text{cm}^{-1}$ . The larger shift ( $\Delta\nu_{\text{OH}} \approx 310 \text{ cm}^{-1}$ ), observed between the free BAS (3616  $\text{cm}^{-1}$ ) and the strongly H-bonded species (3306  $\text{cm}^{-1}$ ), was shown to scale with the BAS strength. Notably, the 3415  $\text{cm}^{-1}$  band was assigned not to less acidic hydroxyls but to different H-bonded configurations of CO on chemically equivalent BAS, as no intrinsic heterogeneity of the acidic OH groups was observed. The authors also clarified that earlier overestimations of  $\Delta\nu_{\text{OH}}$  were caused by Fermi resonance effects, emphasizing that CO provides an accurate probe when analyzed with care. CO adsorption at 80 K on SAPO-34 provides unambiguous spectroscopic evidence of CO–BAS interactions (Figure 2). The O–H stretching modes of the BAS are red shifted from 3630 and 3610  $\text{cm}^{-1}$  to approximately 3350  $\text{cm}^{-1}$ , indicating H-bonded CO–BAS adducts. Concomitantly, the CO stretching mode is blue shifted by 32  $\text{cm}^{-1}$  from CO liquid-like (2138  $\text{cm}^{-1}$ ) [28].

probe accessibility and measured extinction coefficients.

Although the interaction of CO with BAS via H-bonding is weaker than the proton transfer observed with stronger bases (e.g.,  $\text{NH}_3$  or  $\text{C}_5\text{H}_5\text{N}$ ), it nevertheless enables a sensitive assessment of BAS heterogeneity. The low basicity of CO limits site perturbation and minimizes competitive adsorption, making it suitable for probing subtle variations in hydroxyl acidity within zeolites, as reflected by the  $\nu_{\text{CO}}$  and  $\Delta\nu_{\text{OH}}$  values in Table 1 where **zeolite framework codes** (see Glossary) are reported [24].

In principle, the quantification of acid site concentration by CO-FTIR spectra is based on the integrated absorbance of the  $\nu_{\text{C}=\text{O}}$  band and the knowledge of its  $\epsilon$ . However, **reliable and**



Trends In Chemistry

Figure 2. FTIR difference spectra in the O–H (high frequency, 3800–3100  $\text{cm}^{-1}$ ) and in C–O (low frequency, 2220–2040  $\text{cm}^{-1}$ ) stretching region of CO adsorbed at 80 K on SAPO-34 (unpublished data). FTIR: Fourier transform infrared; SAPO-34: a silicoaluminophosphate with CHA structure.

Table 1. Literature FTIR data for CO adsorption on Brønsted and Lewis acid sites of selected zeolites, including  $\nu_{(\text{CO})}$  (or  $\Delta\nu_{(\text{CO})}$ ) and  $\Delta\nu_{(\text{OH})}$

| Material    | Acid site type | $\nu_{(\text{CO})}$ or $\Delta\nu_{(\text{CO})}/\text{cm}^{-1}$ | $\Delta\nu_{(\text{OH})}/\text{cm}^{-1}$ | Refs    |
|-------------|----------------|---|--|---------|
| MFI         | BAS            | 2175 (+32)  | $\approx -310$                           | [24,29] |
| MTT         | BAS            | 2173 (+30)  | $\approx -305$                           | [30]    |
| BEA/MOR     | BAS            | 2165–2178   | –290 to –320                             | [30]    |
| [Al]-SBA-15 | Lewis + BAS    | 2160–2175 (+20–30)  | –250 to –280                             | [23]    |
| FAU         | BAS            | 2171 (+28)  | –234                                     | [31]    |

[Al]-SBA-15: mesoporous ordered silica containing Al; BAS: Brønsted acid sites.

**universally accepted  $\epsilon$  values for CO adsorbed on BAS of zeolites are not available**, as  $\epsilon_{(\text{CO})}$  strongly depends on surface composition, framework topology, temperature, and surface coverage. Reported values span a broad range for CO adsorbed on solids, reflecting the strong sensitivity of the CO vibrational intensity to the local environment and adsorbate–adsorbate interactions [25,28,30]. At sub-monolayer coverages, CO predominantly interacts with isolated acid sites, and the IR response is approximately linear, whereas at higher loadings, dipole–dipole coupling among adjacent CO molecules induces nonlinear absorption behavior and band shifts. Consequently, CO-FTIR is mainly employed for qualitative or semiquantitative analysis of acid strength and site heterogeneity, rather than for absolute quantification of BAS, and careful control of adsorption temperature (typically 77–120 K) and CO pressure is required to remain within the linear regime [23,26]. A reliable quantitative calibration of acid site densities in zeolites has instead been achieved by combining solid-state  $^1\text{H}$  magic-angle spinning nuclear magnetic resonance (MAS NMR) and FTIR spectroscopy. In this approach, Gabrienko *et al.* [30] determined **an  $\epsilon$**  value of  $3.06 \pm 0.04 \text{ cm } \mu\text{mol}^{-1}$  for BAS and  $1.50 \pm 0.06 \text{ cm } \mu\text{mol}^{-1}$  for terminal silanols (Si-OH) in H-ZSM-5 and H-ZSM-23. These values refer to the OH stretching modes and not to the CO vibrations and therefore provide quantitative benchmarks for BAS densities from hydroxyl IR bands. Despite its high sensitivity, CO is not a universal probe. On strongly basic oxides, it may undergo chemical transformations (e.g., carbonate or formyl formation) above  $\sim 150 \text{ K}$ , compromising quantitative interpretation [32]. Moreover, multilayer adsorption or co-adsorption on adjacent acid pairs can result in complex band envelopes requiring careful spectral deconvolution. For this reason, modern studies increasingly combine CO-FTIR with DFT modeling, temperature-programmed desorption (TPD), microcalorimetry, and solid-state NMR to achieve a robust and cross-validated description of acid site density, strength, and heterogeneity [23,27,30,33].

Overall, CO remains a powerful and selective probe of surface acidity owing to its low basicity, molecular simplicity, and well-defined spectroscopic response. Under controlled conditions and alongside complementary methods, CO-FTIR provides reproducible insights into acid strength and site heterogeneity in zeolites and oxides, remaining a benchmark tool for probing acidity in catalysts.

### Deuterated acetonitrile adsorption

Acetonitrile is a small, linear nitrile with a proton affinity of  $788 \text{ kJ mol}^{-1}$  and a kinetic diameter of about  $4.2 \text{ \AA}$  [34], which allows it to access most microporous channels in zeolites [35]. Its proton affinity enables strong interaction with BAS without causing irreversible chemisorption. The polarizable CN produces an intense, well-isolated stretching vibration highly sensitive to H-bonding, making acetonitrile an excellent spectroscopic probe of Brønsted and Lewis acidity [17,35–38].

The detailed interaction of acetonitrile with Brønsted and Lewis acid sites in zeolites was described and interpreted in a study of  $\text{CD}_3\text{CN}$  on HZSM-5 and HY [35].  $\text{CD}_3\text{CN}$  adsorption on BAS produces a characteristic CN band near  $2300\text{ cm}^{-1}$ , whereas adsorption on Lewis sites yields bands at higher frequencies ( $2332\text{--}2320\text{ cm}^{-1}$ ), while interaction with terminal Si-OH gives rise to bands around  $2275\text{ cm}^{-1}$  and gas-phase  $\text{CD}_3\text{CN}$  appears at  $\approx 2265\text{ cm}^{-1}$ . At low coverage,  $\text{CD}_3\text{CN}$  adsorption on bridging OH groups also generates the classical A–B–C trio of OH-related bands at  $\approx 2890, 2400,$  and  $1700\text{ cm}^{-1}$ , well known for strong hydrogen-bonded complexes, whose positions and intensities can be correlated with hydrogen-bond strength and, hence, absolute Brønsted acidity [39].

Deuterated, rather than protonated, acetonitrile is preferred in FTIR studies because the CN region of  $\text{CH}_3\text{CN}$  is complicated by Fermi resonances and combination bands, which obscure and distort the CN fundamental band and complicate baseline definition and band integration [35,40,41]. In  $\text{CD}_3\text{CN}$ , the deuteration of the methyl group shifts CH-related modes sufficiently so that the CN stretching band becomes isolated and narrower, eliminating Fermi resonance with combination bands and greatly simplifying quantitative analysis. Furthermore, the CD stretching/deformation modes appear at lower wavenumbers and with reduced overlap with framework and OH overtones, improving the robustness of deconvolution in the  $2300\text{--}2260\text{ cm}^{-1}$  window, where CN bands associated with distinct site types are found [42]. These spectral advantages are crucial when  $\text{CD}_3\text{CN}$  is used to resolve closely spaced contributions from different acid sites in zeolites (Figure 3).

For the quantitative use of acetonitrile as a Brønsted probe, the key parameter is the  $\epsilon$  of the CN band associated with  $\text{CD}_3\text{CN}$  interacting with BAS. Early work on ferrierite [43] and other zeolites established measured coefficients for hydrogen-bonded  $\text{CD}_3\text{CN}$  in the range of  $2.0$  to  $2.1\text{ cm}^2\text{ }\mu\text{mol}^{-1}$  for the CN band at  $\approx 2297\text{--}2300\text{ cm}^{-1}$  [42]. This value was widely adopted as a framework-independent constant for Brønsted sites, without recalibration, in subsequent studies on zeolite acidity and site heterogeneity, sometimes in combination with higher values

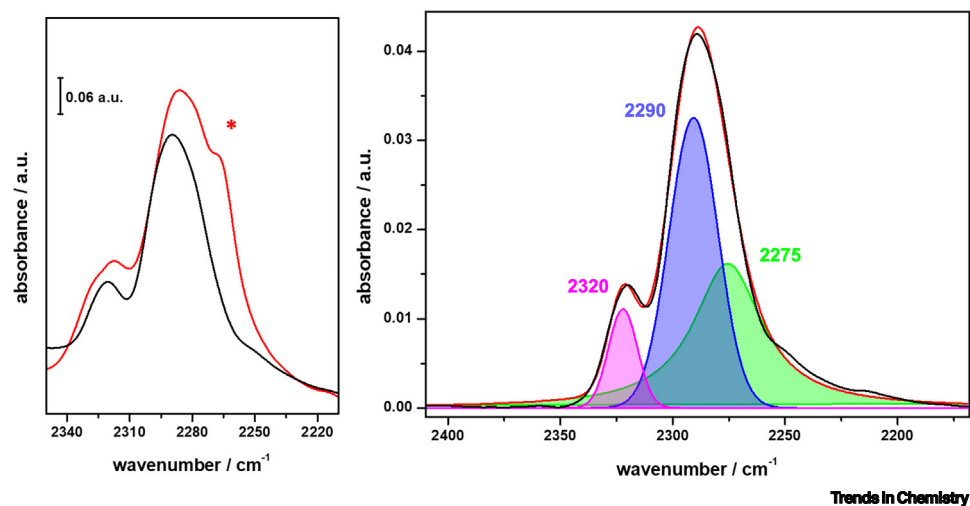


Figure 3. FTIR difference spectra of HFER zeolite at maximum  $\text{d}_3$ -acetonitrile coverage and after desorption of the probe molecules at room temperature (red and black curves, respectively; \*marks the contribution from  $\text{CD}_3\text{CN}$  gas phase). On the right panel, the deconvolution of the irreversible fraction at room temperature is reported, highlighting the different contributions from  $\text{CD}_3\text{CN}$  interacting with Brønsted and Lewis sites; adapted from [42]. FTIR: Fourier transform infrared.; HFER: protonated ferrierite zeolite.

( $\approx 3\text{--}4\text{ cm}^2\ \mu\text{mol}^{-1}$ ) for  $\text{CD}_3\text{CN}$  coordinated to Lewis sites [42–48]. In this ‘first-generation’ approach, then, acetonitrile-based Brønsted site densities were often reported with limited attention to framework dependence or to the stoichiometry linking parent Brønsted sites and newly formed Lewis centers upon partial hydrolysis [17,49].

A recent work has highlighted that  $\epsilon$  values are neither strictly universal nor strictly framework independent; Lebrón-Rodríguez *et al.* proposed a framework-specific recalibration of the  $\text{CD}_3\text{CN}$   $\epsilon$  for BAS in MFI, when partially hydrolyzed and extraframework species have to be precisely accounted [49]. This framework-specific redefinition of  $\epsilon$  represents a significant advancement toward a more accurate determination of molar extinction coefficients and a more quantitatively reliable use of acetonitrile as a Brønsted acid probe. It recognizes that integrated molar coefficients depend on both framework and site identity and that they must be anchored to independent structural metrics by other quantitative methods [ion exchange, inductively coupled plasma (ICP), and NMR].

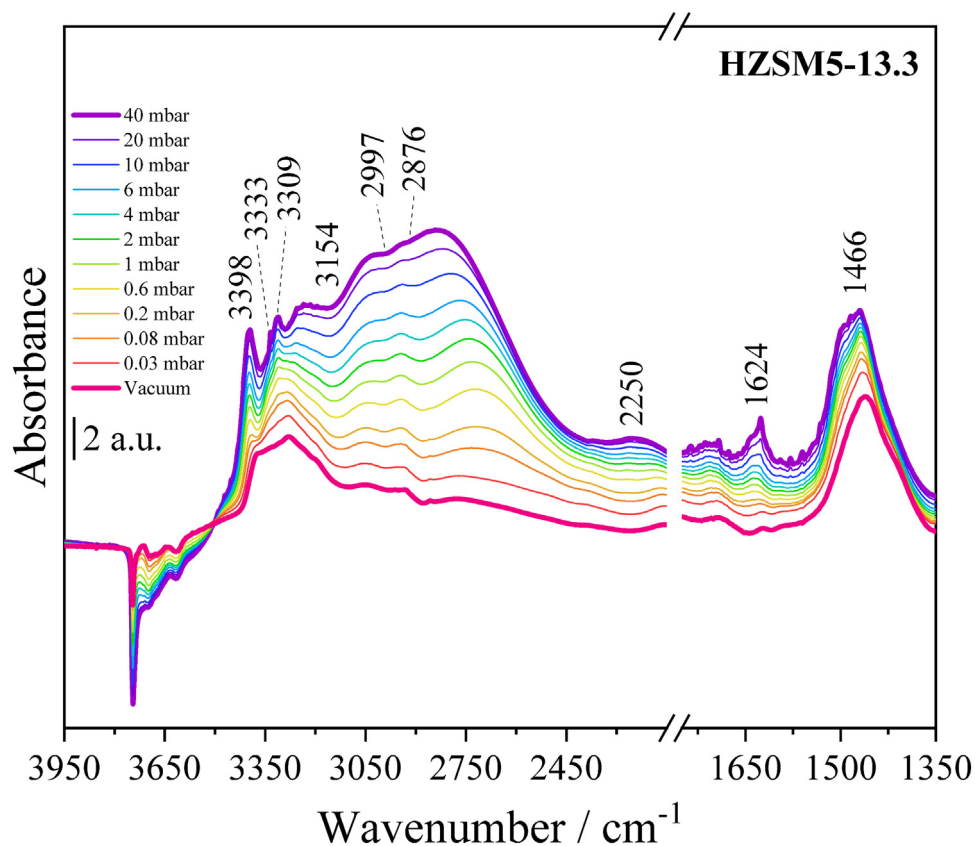
### Ammonia adsorption

$\text{NH}_3$ , a basic molecule with a proton affinity of  $854\text{ kJ mol}^{-1}$ , is widely used as an effective probe molecule for the characterization and quantification of acid sites in porous solids by FTIR spectroscopy. Owing to its small kinetic diameter ( $2.6\text{ \AA}$ ),  $\text{NH}_3$  readily accesses and diffuses through even the narrowest micropores of crystalline frameworks [13]. Beyond its established qualitative use for discriminating acid sites of different strengths,  $\text{NH}_3$  also serves as a semiquantitative tool for determining the concentration of BAS on zeolites. Upon adsorption,  $\text{NH}_3$  interacts with surface species, generating characteristic vibrational features in FTIR spectra [50,51]. Due to  $\text{NH}_3$ 's basicity, in the presence of BAS, a proton transfer mechanism occurs, leading to the formation of the ammonium ion ( $\text{NH}_4^+$ ), which generates a distinctive band at  $\approx 1460\text{ cm}^{-1}$  ( $\delta_{\text{as}}\text{ N-H}$ ) [22,51]. This band is quantitative and can be exploited to estimate BAS concentration via the Lambert–Beer equation adapted for solids [52]. To avoid the contribution of weak probe–surface interactions, it is necessary to carry out the measurements at sufficiently high temperatures ( $\approx 150^\circ\text{C}$ ) [53,54] to prevent  $\text{NH}_3$  physisorption or, alternatively, at room temperature through variable-pressure desorption experiments [22,55]. Upon  $\text{NH}_3$  desorption, bands related to weak acidic site interactions with the probe are completely restored, whereas those associated with BAS remain essentially unchanged due to proton transfer and the  $\text{NH}_4^+$  ions (Figure 4) [55]. Consequently, the characteristic  $\text{NH}_4^+$  band ( $1460\text{ cm}^{-1}$ ) can be unambiguously identified, integrated, and employed for BAS quantification.

The initial  $\text{NH}_3$  pressure strongly affects adsorption equilibrium, influencing both interaction kinetics and diffusion, and should be chosen to maximize interaction with all accessible BAS.

As with other probe molecules, the critical parameter for BAS quantification is the  $\epsilon$  of the ammonium band, which is highly sensitive to the material type, the experimental conditions, and spectral processing, accounting for the variability in reported literature values (Table 2) [56].

In Table 2, all  $\epsilon$  values originate from calibration procedures based on linear correlations between the intensity of the  $\approx 1460\text{ cm}^{-1}$  band and the amount of adsorbed  $\text{NH}_3$ , and the corresponding slopes were used to derive  $\epsilon$ . Most studies rely on reference materials containing exclusively BAS, calculating  $\epsilon$  values upon  $\text{NH}_3$  adsorption [51,53,54,56,57]. Conversely, Bortnovsky *et al.* [58] derived  $\epsilon$  from a linear regression of  $\approx 1460\text{ cm}^{-1}$  band intensities on several zeolites (FER, MOR, MFI, and BEA), obtaining an average coefficient. However, this value was obtained by using  $\text{NH}_4$ -exchanged zeolites. Similarly, Suzuki *et al.* [59] reported an  $\epsilon$  value averaged over multiple zeolite frameworks (MWW, BEA, HY, USY, FER, MFI, and MOR), derived from the



Trends in Chemistry

Figure 4. FTIR difference spectra of  $\text{NH}_3$  adsorbed (max pressure 40 mbar) on hierarchical HZSM5-13.3 sample (HZSM5 desilicated at pH 13.3) at room temperature. The intermediate pressures at which spectra are collected during desorption are reported in the figure; adapted from [55]. FTIR: Fourier transform infrared; HZSM5: protonated ZSM-5 zeolite with MFI structure.

number of BAS and the integrated IR absorption intensity, based on the Lambert–Beer equation, within a combined infrared–mass spectroscopy and temperature-programmed desorption (IRMS–TPD) approach [59]. In addition, sample pretreatment (activation temperature and time) also strongly influences  $\epsilon$  determination, as it affects the removal of residual surface species. In this respect, the literature exhibits a certain degree of inconsistency in the description of activation

Table 2. Selected  $\epsilon$  values for  $\text{NH}_3$  adsorbed on different types of porous materials

| Material   | $\epsilon$ $\text{NH}_3$ -BAS/cm $\mu\text{mol}^{-1}$ | Refs |
|--|---|------|
| FAU  | 0.130   | [51] |
| MOR  | 0.11  | [54] |
| FER  | 14.8  | [56] |
| MCM-41 and modified MCM-41                                     | 3.03  | [57] |
| MCM-41   | 1.47  | [53] |
| $\text{NH}_4$ -zeolites (FER, MOR, MFI, and BEA)               | 13.0  | [58] |
| $\text{NH}_4$ -zeolites (MWW, BEA, HY, USY, FER, MFI, and MOR) | 9.4   | [59] |

procedures, which constitutes a significant limitation for data comparability. All these considerations indicate that  $\text{NH}_3$ -based quantification of BAS sites in zeolites is governed by the concomitant contribution of experimental and methodological factors. These variables act concomitantly and synergistically in defining the uncertainty and heterogeneity of the reported  $\varepsilon$  values, suggesting the presence of a nonnegligible arbitrary component in quantitative measurements.

Consequently,  $\text{NH}_3$ -based BAS probing in zeolites should be regarded as a semiquantitative rather than a strictly quantitative method. Its utility is maximized in comparative studies of the same material under strictly identical experimental conditions, where relative changes and trends can be discerned, and  $\varepsilon$ -related uncertainties mitigated. By contrast, quantitative comparisons across different materials or independent studies remain intrinsically challenging unless all experimental, analytical, and sample-related parameters are rigorously matched. From this perspective, the use of basic probe molecules for acidity characterization constitutes a particularly powerful approach when combined with bulkier probes, as it allows discrimination of BAS accessibility across distinct pore environments, which cannot be resolved by strictly quantitative techniques (Box 2).

### Pyridine adsorption

$\text{C}_5\text{H}_5\text{N}$ , a strong organic base (proton affinity of  $930 \text{ kJ mol}^{-1}$ ), serves as a well-established infrared probe for investigating surface acidity in zeolites [38,65]. Due to its relatively large kinetic diameter ( $5.7 \text{ \AA}$ ),  $\text{C}_5\text{H}_5\text{N}$  is sterically hindered from accessing the internal architecture of small-pore zeolites (e.g., CHA, LTA, and ERI), where narrow apertures ( $\sim 3.8 \text{ \AA}$ ) restrict adsorption to the external surface and pore mouths. While  $\text{C}_5\text{H}_5\text{N}$  effectively distinguishes Brønsted and

#### Box 2. Probing and quantifying accessibility of acidic sites

Accessibility, and not only the number and strength of BAS, is crucial for the catalytic effectiveness of zeolites. Due to their microporous structure, many internal sites are inaccessible to bulky molecules, limiting the catalytic performances, especially in terms of reusability. Enhancing accessibility, for example, through mesopores generation, can improve accessibility and extend the applicability of zeolites to the catalytic processing of bulky reactants.

IR investigation with probe molecules of different kinetic diameter is a powerful tool to assess accessibility. Small probes such as  $\text{NH}_3$  ( $\sim 0.26 \text{ nm}$ ) access almost all acid sites, whereas larger probes, such as 2,4,6-trimethylpyridine ( $\sim 0.74 \text{ nm}$ ), 2,6-di-tert-butylpyridine ( $\sim 0.83 \text{ nm}$ ), 2,4,6-tri-tert-butylpyridine ( $\sim 1.1 \text{ nm}$ ), and trihexylamine ( $\sim 1.4 \text{ nm}$ ), cannot enter most micropores and thus selectively probe acid sites on external surfaces [60,61] or in mesopores [62]. In 2009, Thibault-Starzyk *et al.* [63] introduced a key method to quantify acid site accessibility in hierarchical zeolites. At the time, such materials, combining zeolitic microporosity ( $0.25\text{--}1 \text{ nm}$ ) with a secondary mesopore network ( $2\text{--}50 \text{ nm}$ ), were recognized for overcoming the diffusion limits of purely microporous zeolites. However, evidence of improved site accessibility was mostly indirect, and no standardized quantitative protocol existed to directly assess it across materials prepared by different routes. This gap hindered rational catalyst design by preventing correlation between structure, transport, and catalytic performance. To address it, the authors proposed the accessibility index (AI) or accessibility factor (AF), defined as the ratio of acid sites titrated by a bulky probe to those detected by a small one (e.g.,  $\text{NH}_3$ ).

When evaluating Lewis acid sites, this approach is generally reliable, whereas for Brønsted sites, additional caution is required. Protons from Brønsted hydroxyl groups may be drawn toward strong bases even from sterically protected regions, allowing interaction with hydroxyl groups in regions considered virtually inaccessible and complicating accessibility assessment [10].

Ideally, reactant molecules themselves should be used to probe accessibility; nevertheless, this is often not possible, so careful probe selection is essential. The use of too bulky probes can underestimate accessibility, while, for correlating accessibility with catalytic outcomes, the probe must be chosen considering both size and chemical properties of reactants [64]. The size of the chosen probe molecule, in fact, should be comparable to the steric hindrance of the reactant, to specifically probe the fraction of acid sites relevant for a given reaction.

Lewis acid sites, its molecular sieving effect can underestimate total acidity in small-pore zeolites compared to smaller probes like  $\text{NH}_3$ . This limitation is often used to differentiate external from internal acidity. Whereas small molecules assess total acidity in zeolites,  $\text{C}_5\text{H}_5\text{N}$  provides a specific map of the acid sites available for bulkier catalytic reactants, which are subject to the same diffusion constraints (Box 2).

$\text{C}_5\text{H}_5\text{N}$  can be adsorbed on surface sites of solids through different interaction modes, depending on the nature and strength of these sites. This effect is clearly reflected in the vibrational ring modes of the molecule ( $\nu_{8a}$ ,  $\nu_{8b}$ ,  $\nu_{19a}$ , and  $\nu_{19b}$ ), which occur in the  $1700\text{--}1400\text{ cm}^{-1}$  IR region.  $\text{C}_5\text{H}_5\text{N}$  can be weakly physisorbed or H-bonded to surface Si-OH, giving rise to bands at  $1595$  and  $1580\text{ cm}^{-1}$  ( $\nu_{8a}$  and  $\nu_{8b}$ ) and  $1445$  and  $1438\text{ cm}^{-1}$  ( $\nu_{19a}$  and  $\nu_{19b}$ ). In contrast,  $\text{C}_5\text{H}_5\text{N}$  coordination to Lewis sites leads to typical bands at  $1456\text{ cm}^{-1}$  ( $\nu_{19b}$ ) and  $1622\text{ cm}^{-1}$  ( $\nu_{8a}$ ). Finally, when  $\text{C}_5\text{H}_5\text{N}$  is adsorbed on BAS in zeolites (Figure 5), proton transfer occurs, leading to the formation of pyridinium ions ( $\text{PyH}^+$ ), which exhibit characteristic ring modes at  $1635$  and  $1623\text{ cm}^{-1}$  ( $\nu_{8a}$  and  $\nu_{8b}$ ) and at  $1545$  and  $1488\text{ cm}^{-1}$  ( $\nu_{19b}$  and  $\nu_{19a}$ ) [20,66].

To specifically monitor the formation of pyridinium ions, which reflect the BAS concentration, the zeolite is outgassed at approximately  $150^\circ\text{C}$  to remove weakly adsorbed  $\text{C}_5\text{H}_5\text{N}$  from the FTIR spectra. Subsequently, the BAS quantification is commonly performed by integrating the  $1545\text{ cm}^{-1}$  band, as it does not overlap with other ring vibrational bands. However, accurate quantification of the  $\epsilon$  remains challenging, as the literature reports a wide range of  $\epsilon$  values for  $\text{C}_5\text{H}_5\text{N}$  adsorbed on BAS (Py-BAS) in FAU, MOR, MFI, and BEA zeolites (Table 3) [20,70].

An accurate determination of the  $\epsilon$  of  $\text{C}_5\text{H}_5\text{N}$  adsorbed on BAS in zeolites has recently been reported by combining FTIR spectroscopy with high-precision thermogravimetric analysis

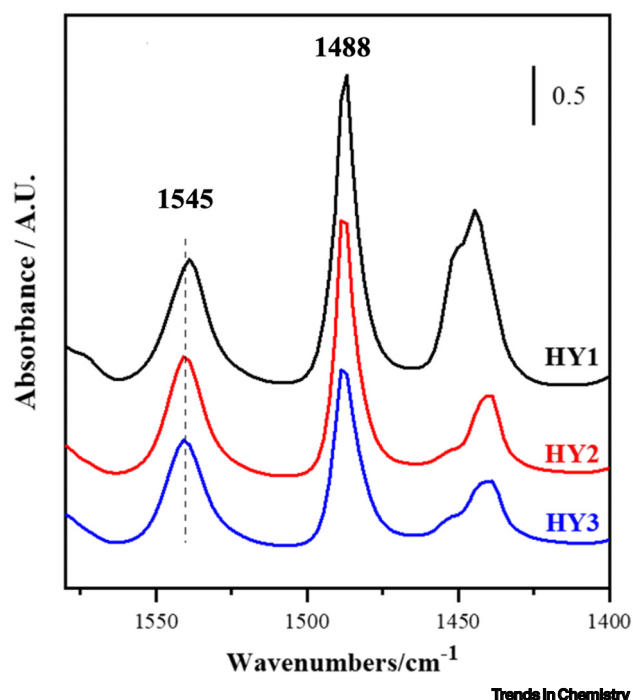


Figure 5. FTIR difference spectra of adsorbed  $\text{C}_5\text{H}_5\text{N}$  on HY zeolites with different porous distribution upon outgassing the sample at  $150^\circ\text{C}$ ; adapted from [64]. FTIR: Fourier transform infrared.

Table 3. Selected  $\epsilon$  values for  $C_5H_5N$  adsorbed on different zeolites

| Material | $\epsilon$ (Py-BAS)               | Units                | Temperature/ $^{\circ}C$ | Refs |
|----------|-----------------------------------|----------------------|--------------------------|------|
| FAU      | 0.73                              | $cm\ \mu mol^{-1}$   | 200                      | [67] |
|          | $1.67 \pm 0.12$                   | $cm\ \mu mol^{-1}$   | 150                      | [9]  |
|          | $1.8 \pm 0.1$                     | $cm\ \mu mol^{-1}$   | -                        | [68] |
|          | $0.078 \pm 0.004$                 | $cm^2\ \mu mol^{-1}$ | 145                      | [69] |
|          | $1.36 \pm 0.03$                   | $cm\ \mu mol^{-1}$   | 200                      | [21] |
|          | $1.95 \pm 0.13$                   | $cm\ \mu mol^{-1}$   | 150                      | [40] |
|          | <b><math>1.54 \pm 0.15</math></b> | $cm\ \mu mol^{-1}$   | 150                      | [20] |
|          | <b><math>1.46 \pm 0.15</math></b> | $cm\ \mu mol^{-1}$   | 200                      | [20] |
| MOR      | $1.67 \pm 0.12$                   | $cm\ \mu mol^{-1}$   | 150                      | [9]  |
|          | 1.8                               | $cm\ \mu mol^{-1}$   | 30                       | [70] |
|          | $0.078 \pm 0.004$                 | $cm^2\ \mu mol^{-1}$ | 145                      | [69] |
|          | <b><math>1.29 \pm 0.04</math></b> | $cm\ \mu mol^{-1}$   | 150                      | [20] |
|          | <b><math>1.23 \pm 0.04</math></b> | $cm\ \mu mol^{-1}$   | 200                      | [20] |
|          |                                   |                      |                          |      |
| MFI      | $1.67 \pm 0.12$                   | $cm\ \mu mol^{-1}$   | 150                      | [9]  |
|          | 0.07                              | $cm^2\ \mu mol^{-1}$ | 170                      | [71] |
|          | $1.3 \times 10^{-6}$              | $cm\ \mu mol^{-1}$   | 150                      | [72] |
|          | <b><math>1.09 \pm 0.08</math></b> | $cm\ \mu mol^{-1}$   | 150                      | [20] |
|          | <b><math>1.05 \pm 0.08</math></b> | $cm\ \mu mol^{-1}$   | 200                      | [20] |
|          |                                   |                      |                          |      |
| BEA      | 1.38                              | $cm\ mmol^{-1}$      | 150                      | [73] |
|          | $1.3 \times 10^{-6}$              | $cm\ \mu mol^{-1}$   | 30                       | [74] |
|          | 0.070                             | $cm\ \mu mol^{-1}$   | 150                      | [75] |
|          | <b><math>1.12 \pm 0.16</math></b> | $cm\ \mu mol^{-1}$   | 150                      | [20] |
|          | <b><math>1.07 \pm 0.15</math></b> | $cm\ \mu mol^{-1}$   | 200                      | [20] |

Py-BAS: pyridine adsorbed on BAS

(AGIR), enabling the simultaneous measurement of sample mass (corresponding to adsorbed  $C_5H_5N$ ) and IR band intensities [20]. This methodology significantly reduces the uncertainties commonly associated with conventional quantification approaches. The calculated  $\epsilon$  values depend systematically on multiple parameters, including the zeolite framework,  $C_5H_5N$  desorption temperature, IR spectral resolution, and pellet density. As a result, reliable and comparable quantification critically requires the standardization of experimental protocols. Complete removal of physisorbed  $C_5H_5N$  is essential, as residual weakly bound species can induce solvent-like effects that attenuate the Py-BAS vibrational band. The framework-dependent nature of the response further emphasizes the need for structure-specific calibration coefficients rather than reliance on nominally universal literature values. In addition, because  $\epsilon$  is temperature sensitive, sample temperature must be controlled and clearly reported to allow reliable comparison between studies. Notably,  $\epsilon$  values increase in the order ZSM-5/BEA < MOR < FAU, a trend attributed to differences in Si/Al ratio, acid strength, and confinement effects within the zeolite micropores. The experimental  $\epsilon$  values for the various zeolite frameworks, obtained in this reference study and highlighted in bold in Table 3, provide a robust and transferable benchmark for the quantitative assessment of Brønsted acidity in zeolites using  $C_5H_5N$  as a probe molecule. Their reliability is further reinforced by recent literature reports that have applied these  $\epsilon$  values to the quantitative determination of BAS in zeolite Y [60].

### How the choice of extinction coefficient shapes BAS quantification

To better illustrate the implications arising from the use of different molar extinction coefficients, even when considering the same material, a representative experimental dataset can be reprocessed using alternative  $\epsilon$  values. In the case of BAS quantification using  $C_5H_5N$  as a probe molecule, Zholobenko *et al.* [20] reported BAS concentrations of 325 and 450  $\mu\text{mol g}^{-1}$  for ZSM-5-40 and ZSM-5-27 (MFI framework), respectively. In that work, the molar extinction coefficient ( $\epsilon$ ) was determined through an advanced methodology combining gravimetric analysis with FTIR spectroscopy, yielding a value of 1.09  $\text{cm } \mu\text{mol}^{-1}$ . If, instead, the same integrated absorbances were reprocessed—under identical assumptions regarding material and experimental conditions—using the value proposed by Emeis [9] ( $\epsilon = 1.67 \text{ cm } \mu\text{mol}^{-1}$ ), a substantial variation in the calculated BAS concentration would be obtained. Notably, Emeis originally reported no evidence for a dependence of the integrated molar extinction coefficients (IMECs) on either catalyst structure or strength of the acid site. Under this alternative assumption, the BAS concentrations would decrease to 212 and 294  $\mu\text{mol g}^{-1}$  for ZSM-5-40 and ZSM-5-27, respectively, corresponding to a reduction of approximately 35%.

An analogous approach can be applied to  $NH_3$ -based quantification. Suzuki *et al.* [59] reported a BAS concentration of 420  $\mu\text{mol g}^{-1}$  for an MFI zeolite (Si/Al = 46), employing an averaged extinction coefficient of 9.4  $\text{cm } \mu\text{mol}^{-1}$  (Table 2). Reprocessing the same data using an alternative averaged value of  $\epsilon = 13.0 \text{ cm } \mu\text{mol}^{-1}$ , as proposed by Bortnovsky *et al.* [58], would lead to a recalculated BAS concentration of 304  $\mu\text{mol g}^{-1}$ , that is, approximately 28% lower.

These examples represent illustrative recalculations based on hypothetical reprocessing of the same experimental data using different  $\epsilon$  values, aimed at highlighting the strong impact of the chosen extinction coefficient on the derived BAS concentration.

### Concluding remarks

FTIR spectroscopy combined with probe-molecule adsorption is a powerful and versatile tool for investigating acidity in solid catalysts, especially zeolites, as it allows the identification and characterization of BAS, which are crucial for understanding their catalytic behavior.

Beyond qualitative identification, the quantitative analysis of BAS in zeolites critically depends on methodological rigor, with particular emphasis on the determination of reliable molar extinction coefficients and strict control of experimental parameters such as sample preparation, adsorption conditions, temperature, and spectral normalization.

The wide variability of  $\epsilon$  values in the literature complicates comparisons across solids, making careful evaluation of how these coefficients were obtained key to the realistic quantification of acid sites. Combining small probes (e.g., CO and  $NH_3$ ) for total site mapping with bulkier probes (e.g.,  $C_5H_5N$ ) for pore-specific assessment enables a comprehensive understanding of site accessibility and heterogeneity. When coupled with standardized protocols and rigorously calibrated  $\epsilon$  values, probe-molecule FTIR studies provide robust structure–property relationships, guiding the rational design of selective, efficient, and sustainable catalysts. Importantly, the technique becomes truly quantitative when integrated with temperature-programmed studies or solid-state NMR, providing robust structure–property correlations and guiding the rational design of next-generation catalysts for sustainable and green chemistry applications (see Outstanding questions).

### Outstanding questions

Is there a reliable strategy to standardize  $\epsilon$  values across different laboratories while explicitly accounting for differences in pellet preparation, scattering effects, spectral resolution, and temperature-dependent band intensities?

Can unified cross-calibration workflows, combining Fourier transform infrared with quantitative techniques (e.g., magic-angle spinning nuclear magnetic resonance, gravimetry, or infrared-mass spectroscopy and temperature-programmed desorption), be translated into standardized and widely adoptable protocols for framework- and site-specific  $\epsilon$  determination?

How should mixed Brønsted/Lewis acidity populations and the possible formation of extra-framework Al species be accounted for in the overall acidity quantification when using basic probes for zeolite characterization?

How can probe-size-dependent Fourier transform infrared approaches be made more robust and standardized to reliably discriminate between internal and external Brønsted acid sites in hierarchical and small-pore zeolites?

Can operando and variable-temperature Fourier transform infrared measurements under reactive gas feeds deliver quantitative, time-resolved acidity information without losing comparability with established vacuum-based reference protocols?

Can Brønsted acid site quantification, based on different molecular probes, be organized into a common quantitative scale through well-defined conversion or normalization procedures to enable consistent comparison of materials?

Can differences in Brønsted acid site concentrations, derived from different basic probes, be rationalized by integrating information on pore size distributions obtained from porosimetric analyses with the aid of the most suitable density functional theory models?

## Acknowledgments

Dr Gioele Ancora holds a PhD career grant supported by NextGenerationEU-MUR.

This work was funded by the European Union—NextGenerationEU, Mission 4, Component 1, CUP 20224C35S7\_002.

## Declaration of interests

The authors declare no competing interests.

## Declaration of Generative AI and AI-assisted technologies in the writing process

During the preparation of this manuscript, the authors used ChatGPT (Open AI) to reduce the number of words as required by the guidelines. After using this tool, the authors reviewed and edited the content as needed and take full responsibility for the content of the published article.

## References

1. Friend, C.M. and Xu, B. (2017) Heterogeneous catalysis: a central science for a sustainable future. *Acc. Chem. Res.* 50, 517–521
2. Vogt, C. and Weckhuysen, B.M. (2022) The concept of active site in heterogeneous catalysis. *Nat. Rev. Chem.* 6, 89–111
3. Zaera, F. (2022) Designing sites in heterogeneous catalysis: are we reaching selectivities competitive with those of homogeneous catalysts? *Chem. Rev.* 122, 8594–8757
4. Anastas, P.T. and Warner, J.C. (2000) *Green Chemistry: Theory and Practice*, Oxford University Press
5. Pham, T.N. *et al.* (2023) Influence of Brønsted acid site proximity on alkane cracking in MFI zeolites. *ACS Catal.* 13, 1359–1370
6. Cnudde, P. *et al.* (2020) Light olefin diffusion during the MTO process on H-SAPO-34: a complex interplay of molecular factors. *J. Am. Chem. Soc.* 142, 6007–6017
7. Cnudde, P. *et al.* (2021) Experimental and theoretical evidence for the promotional effect of acid sites on the diffusion of alkenes through small-pore zeolites. *Angew. Chem. Int. Ed.* 60, 10016–10022
8. Trachta, M. *et al.* (2023) Investigation of Brønsted acidity in zeolites through adsorbates with diverse proton affinities. *Sci. Rep.* 13, 12380
9. Emeis, C.A. (1993) Determination of integrated molar extinction coefficients for infrared absorption bands of pyridine adsorbed on solid acid catalysts. *J. Catal.* 141, 347–354
10. Lercher, J.A. *et al.* (1996) Infrared studies of the surface acidity of oxides and zeolites using adsorbed probe molecules. *Catal. Today* 27, 353–376
11. Zhang, H. *et al.* (2022) Zeolites in catalysis: sustainable synthesis and its impact on properties and applications. *Catal. Sci. Technol.* 12, 6024–6039
12. Liu, Q. and van Bokhoven, J.A. (2024) Water structures on acidic zeolites and their roles in catalysis. *Chem. Soc. Rev.* 53, 3065–3095
13. Giordano, F. *et al.* (2014) Interaction of NH<sub>3</sub> with Cu-SSZ-13 catalysts: a complementary FTIR, XANES, and XES study. *J. Phys. Chem. Lett.* 5, 1552–1559
14. Chizallet, C. *et al.* (2023) Molecular views on mechanisms of Brønsted acid-catalyzed reactions in zeolites. *Chem. Rev.* 123, 6107–6196
15. Graziano, G. (2017) Heterogeneous catalysis: À la carte zeolites. *Nat. Rev. Chem.* 1, 0037
16. Morterra, C. *et al.* (2001) On the critical use of molar absorption coefficients for adsorbed species: the methanol/silica system. *Catal. Today* 70, 43–58
17. Bordiga, S. *et al.* (2015) Probing zeolites by vibrational spectroscopies. *Chem. Soc. Rev.* 44, 7262–7341
18. Jentoft, F.C. *et al.* (2013) Quantitative analysis of IR intensities of alkanes adsorbed on solid acid catalysts. *J. Phys. Chem. C* 117, 5873–5881
19. Glorius, M. *et al.* (2020) Determination of extinction coefficients for describing gas adsorption on heterogeneous catalysts using in-situ DRIFT spectroscopy. *Catalysts* 10, 735
20. Zholobenko, V. *et al.* (2020) Probing the acid sites of zeolites with pyridine: quantitative AGR measurements of the molar absorption coefficients. *J. Catal.* 385, 52–60
21. Thibault-Starzyk, F. *et al.* (2004) In situ thermogravimetry in an infrared spectrometer: an answer to quantitative spectroscopy of adsorbed species on heterogeneous catalysts. *Microporous Mesoporous Mater.* 67, 107–112
22. Erigoni, A. *et al.* (2019) Acid properties of organosiliceous hybrid materials based on pendant (fluoro)aryl-sulfonic groups through a spectroscopic study with probe molecules. *Catal. Sci. Technol.* 9, 6308–6317
23. Gallo, J.M.R. *et al.* (2010) Physicochemical characterization and surface acid properties of mesoporous [Al]-SBA-15 obtained by direct synthesis. *Langmuir* 26, 5791–5800
24. Chakarova, K. and Hadjivanov, K. (2011) H-bonding of zeolite hydroxyls with weak bases: FTIR study of CO and N<sub>2</sub> adsorption on H-D-ZSM-5. *J. Phys. Chem. C* 115, 4806–4817
25. Corma, A. (1997) Solid acid catalysts. *Curr. Opin. Solid State Mater. Sci.* 2, 63–75
26. Hadjivanov, K. *et al.* (1996) IR study of CO adsorption on Cu-ZSM-5 and CuO/SiO<sub>2</sub> catalysts:  $\sigma$  and  $\pi$  components of the Cu<sup>+</sup>-CO bond. *J. Chem. Soc. Faraday Trans.* 92, 4595–4600
27. Maleki, F. and Pacchioni, G. (2020) Characterization of acid and basic sites on zirconia surfaces and nanoparticles by adsorbed probe molecules: a theoretical study. *Top. Catal.* 63, 1717–1730
28. Miletto, I. *et al.* (2017) Mesoporous silica scaffolds as precursor to drive the formation of hierarchical SAPO-34 with tunable acid properties. *Chem. Eur. J.* 23, 9952–9961
29. Wakabayashi, F. *et al.* (1995) Direct comparison of N<sub>2</sub> and CO as IR-spectroscopic probes of acid sites in H-ZSM-5 zeolite. *J. Phys. Chem.* 99, 10573–10580
30. Gabrienko, A.A. *et al.* (2018) Direct measurement of zeolite Brønsted acidity by FTIR spectroscopy: solid-state <sup>1</sup>H MAS NMR approach for reliable determination of the integrated molar absorption coefficients. *J. Phys. Chem. C* 122, 25386–25395
31. Chakarova, K. *et al.* (2016) FTIR study of CO and N<sub>2</sub> adsorption on [Ge]FAU zeolites in their Na- and H-forms. *Microporous Mesoporous Mater.* 220, 188–197
32. Abbas-Ghaleb, R. (2020) Boron alumina: qualitative investigation of the surface acidity by FTIR measurements of CO adsorption. *SN Appl. Sci.* 2, 2154
33. Butova, V.V. *et al.* (2023) In situ FTIR spectroscopy for scanning accessible active sites in defect-engineered UiO-66. *Nanomaterials (Basel)* 13, 1675
34. Palčić, A. and Valtchev, V. (2020) Analysis and control of acid sites in zeolites. *Appl. Catal. A Gen.* 606, 117795
35. Angell, C.L. and Howell, M.V. (1969) Infrared spectroscopic investigation of zeolites and adsorbed molecules. IV. Acetonitrile. *J. Phys. Chem.* 73, 2551–2554
36. Pelmenchikov, A.G. *et al.* (1993) Acetonitrile-d<sub>3</sub> as a probe of Lewis and Brønsted acidity of zeolites. *J. Phys. Chem.* 97, 11071–11074
37. Paniagua, M. *et al.* (2021) Understanding the role of Al/Zr ratio in Zr-Al-beta zeolite: towards the one-pot production of GVL from glucose. *Catal. Today* 367, 228–238
38. Hadjivanov, K. (2014) Chapter Two - Identification and Characterization of Surface Hydroxyl Groups by Infrared Spectroscopy. In *Advances in Catalysis* (57) (Friederike C. Jentoft, , ed.), pp.

- 99–318, Academic Press - Elsevier, University of Oklahoma, Norman, Oklahoma, USA
39. Pelmeshnikov, A.G. *et al.* (1995) (A,B,C) Triplet of infrared OH bands of zeolitic H-complexes. *J. Phys. Chem.* 99, 3612–3617
40. Harris, J.W. *et al.* (2016) Titration and quantification of open and closed Lewis acid sites in Sn-Beta zeolites that catalyze glucose isomerization. *J. Catal.* 335, 141–154
41. Venkateswarlu, P. (1951) The rotation-vibration spectrum of methyl cyanide in the region 1.6 $\mu$ –20 $\mu$ . *J. Chem. Phys.* 19, 293–298
42. Milletto, I. *et al.* (2018) In situ FT-IR characterization of CuZnZr/ferrierite hybrid catalysts for one-pot CO<sub>2</sub>-to-DME conversion. *Materials (Base)* 11, 2275
43. Wichterlová, B. *et al.* (1998) Determination and properties of acid sites in H-ferrierite: a comparison of ferrierite and MFI structures. *Microporous Mesoporous Mater.* 24, 223–233
44. Medak, G. *et al.* (2023) The influence of inserted metal ions on acid strength of OH groups in Faujasite. *Crystals* 13, 332
45. Taylor, R. *et al.* (2016) Molecular interactions in crystal structures with Z' > 1. *Cryst. Growth Des.* 16, 2988–3001
46. Katada, N. *et al.* (2022) Acidic property of YNU-5 zeolite influenced by its unique micropore system. *Microporous Mesoporous Mater.* 330, 111592
47. Čejka, J. *et al.* (2002) Activity and selectivity of zeolites MCM-22 and MCM-58 in the alkylation of toluene with propylene. *Microporous Mesoporous Mater.* 53, 121–133
48. Hebisch, K.L. *et al.* (2024) Synergy between Bronsted acid sites and carbonaceous deposits during skeletal 1-butene isomerization over ferrierite. *ACS Catal.* 14, 10280–10294
49. Lebrón-Rodríguez, E.A. *et al.* (2025) Quantifying site heterogeneity in microporous aluminosilicates and implications for catalysis. *ACS Catal.* 15, 17314–17332
50. Sadowska, K. *et al.* (2013) Desilication of highly siliceous zeolite ZSM-5 with NaOH and NaOH/tetrabutylamine hydroxide. *Microporous Mesoporous Mater.* 168, 195–205
51. Gackowski, M. *et al.* (2019) IR and NMR studies of the status of Al and acid sites in desilicated zeolite Y. *Molecules* 25, 31
52. Zecchina, A. *et al.* (1997) Vibrational spectroscopy of NH<sub>4</sub><sup>+</sup> ions in zeolitic materials: an IR study. *J. Phys. Chem. B* 101, 10128–10135
53. Taouli, A. *et al.* (1999) Acidity investigations and determination of integrated molar extinction coefficients for infrared absorption bands of ammonia adsorbed on acidic sites of MCM-41. *Stud. Surf. Sci. Catal.* 125, 307–314
54. Góra-Marek, K. *et al.* (2005) IR and NMR studies of mesoporous alumina and related aluminosilicates. *Catal. Today* 101, 131–138
55. Ancora, G. *et al.* (2025) Insights into the role of hierarchical porosity in zeolite architectures for selective uptake of metal ions in solution. *RSC Adv.* 15, 20092–20110
56. Datka, J. *et al.* (2003) Acid properties of NaKH-ferrierites of various exchange degrees studied by IR spectroscopy. *Appl. Catal. A Gen.* 243, 293–299
57. Taouli, A. and Reschetilowski, W. (2002) Comparative study of MCM-41 acidity by using the integrated molar extinction coefficients for infrared absorption bands of adsorbed ammonia. *Stud. Surf. Sci. Catal.* 142, 1315–1322
58. Bortnovsky, O. *et al.* (2001) Quantitative analysis of aluminum and iron in the framework of zeolites. *Microporous Mesoporous Mater.* 42, 97–102
59. Suzuki, K. *et al.* (2007) IRMS-TPD of ammonia: direct and individual measurement of Bronsted acidity in zeolites and its relationship with the catalytic cracking activity. *J. Catal.* 250, 151–160
60. Rejman, S. *et al.* (2025) External acidity as performance descriptor in polyolefin cracking using zeolite-based materials. *Nat. Commun.* 16, 2980
61. Beutel, T.W. *et al.* (2021) Probing external Bronsted acid sites in large pore zeolites with infrared spectroscopy of adsorbed 2,4,6-tri-tert-butylpyridine. *J. Phys. Chem. C* 125, 8518–8532
62. Han, Y. *et al.* (2025) On the use of a bulky base for evaluating the accessibility of Bronsted acid sites in USY zeolites. *Microporous Mesoporous Mater.* 397, 113746
63. Thibault-Starzyk, F. *et al.* (2009) Quantification of enhanced acid site accessibility in hierarchical zeolites – the accessibility index. *J. Catal.* 264, 11–14
64. Yang, P. *et al.* (2025) The effect of accessibility to acid sites in Y zeolites on ring opening reaction in light cycle oil hydrocracking. *Chem. Synth.* 5, 24–40
65. Dalena, F. *et al.* (2024) Evaluation of zeolite composites by IR and NMR spectroscopy. *Molecules* 29, 4450
66. Gould, N.S. and Xu, B. (2018) Quantification of acid site densities on zeolites in the presence of solvents via determination of extinction coefficients of adsorbed pyridine. *J. Catal.* 358, 80–88
67. Datka, J. (1992) Acidic properties of supported niobium oxide catalysts: an infrared spectroscopy investigation. *J. Catal.* 135, 186–199
68. Khabtoui, S. *et al.* (1994) Quantitative infrared study of the distinct acidic hydroxyl groups contained in modified Y zeolites. *Microporous Mater.* 3, 133–148
69. Datka, J. *et al.* (1996) Heterogeneity of OH groups in H-mordenites: effect of dehydroxylation. *Zeolites* 17, 428–433
70. Maache, M. *et al.* (1995) FT infrared study of Bronsted acidity of H-mordenites: heterogeneity and effect of dealumination. *Zeolites* 15, 507–516
71. Tarach, K.A. *et al.* (2017) Acidity and accessibility studies of desilicated ZSM-5 zeolites in terms of their effectiveness as catalysts in acid-catalyzed cracking processes. *Catal. Sci. Technol.* 7, 858–873
72. Take, J. *et al.* (1986) Bronsted site population on external and on internal surface of shape-selective catalysts. *Stud. Surf. Sci. Catal.* 28, 495–502
73. Park, H. *et al.* (2024) Assessment of acid catalytic properties of ferrosilicate MFI zeolite by methanol-to-hydrocarbon conversion. *RSC Adv.* 14, 29006–29013
74. Kiricsi, I. *et al.* (1994) Progress toward understanding zeolite  $\beta$  acidity: an IR and 27Al NMR spectroscopic study. *J. Phys. Chem.* 98, 4627–4634
75. Góra-Marek, K. *et al.* (2006) Influence of V content on the nature and strength of acidic sites in VSi $\beta$  zeolite evidenced by IR spectroscopy. *J. Phys. Chem. B* 110, 6763–6767